

Structural vibration transmission in stiffened structures

James A. Forrest

Maritime Platforms Division, Defence Science & Technology Organisation, 506 Lorimer St, Fishermans Bend VIC 3207, Australia.

ABSTRACT

Plates and shells with beam stiffeners are common structural elements in ships, aircraft and land vehicles. Several approaches can be used to model the dynamics of these elements. One is to smear the mass and stiffness of the beam stiffeners to give an orthotropic plate or shell which models the low-frequency response well. Another is the use of periodic structure theory to give a compact result for the vibration transmission with evenly spaced stiffeners considered discretely. This paper considers a cylindrical shell with ring stiffeners as an example problem and compares the performance of the smeared model with that of the discrete-stiffener approach. A method that could be used to investigate the effect of some randomisation in stiffener spacing is also described.

INTRODUCTION

Plates and shells are basic structural building blocks and their dynamics have been of interest since the earliest investigations in mechanics. Stiffeners in the form of beams of various cross-sections are used in many plate and shell structures to increase stiffness and strength with a minimal increase in weight. Earlier work on stiffened plates and stiffened cylindrical shells is described by Leissa (1993a, 1993b). These approaches treat the stiffened structure as an equivalent orthotropic one, i.e. the stiffeners' mass and stiffness is effectively smeared over the continuous plate or shell. As noted by Leissa (1993b) and compared by Ruotolo (2002), there are a number of thin-shell theories, which differ in the terms included to account for shell bending.

The advantage of smearing the stiffener properties is that it makes the solution of the plate or shell dynamics only a little more complicated than the uniform isotropic case. Gan *et al.* (2009) apply the smeared approach in a wave propagation method to solve the natural frequencies of a ring-stiffened cylindrical shell. Luan *et al.* (2011) propose improvements to the smeared approximation for cross-stiffened rectangular plates. Beyond simple smearing, Junger and Feit (1993) consider reaction forces on a plate due to just the translational and rotary inertia of regularly spaced stiffeners.

Large structures with evenly spaced stiffeners can be analysed as infinite periodic structures. Consideration of structural periodicity results in pass and stop bands of vibration transmission which are not accounted for in smeared-stiffener analysis. Mace (1980) considers infinite fluid-loaded stiffened plates excited by line and point forces, giving general expressions for the stiffener reaction forces and moments and specific values for beam-like stiffeners. Langley (1989) applies the periodic method to a chain of plates joined end to end, each with two sides simply supported and a stiffener at the joins. He also discusses the use of the dynamic-stiffness matrix for a single plate unit in assembling a structure with varied stiffener spacing from a finite number of plate units. Hodges *et al.* (1985) model an infinitely long ring-stiffened cylindrical shell using Fourier decomposition and space-harmonic analysis, with the cross-section of the symmetric stiffeners allowed to distort. Mead and Bardell (1986) inves-

tigate wave propagation in a cylinder with axial stiffeners (stringers), and, in Mead and Bardell (1987), in a cylinder with circumferential (ring) stiffeners. They allow for stiffeners of arbitrary cross-section. The approach assumes periodicity in the circumferential or axial direction respectively, and seeks propagation constants that are related to the wave types in the cylinder. They note that either axial or circumferential stiffeners can be considered with this method, but not both together. Lee and Kim (2002) apply a similar method for sound transmission through a ring-stiffened aircraft fuselage, but treat each stiffener as a lumped mass, translational spring and rotational spring. Efimtsov and Lazarev (2009) demonstrate a solution for periodically stiffened plates and shells using space-harmonic expansions which is more amenable at high frequencies than the propagation constant method. Solaroli *et al.* (2003) analyse periodically stiffened shells numerically using the finite-element method.

A cylindrical shell with ring stiffeners will be considered in this paper. Such shells are of practical interest in many applications. A cylindrical shell is equivalent to a plate rolled up, but the introduction of the curvature couples all three displacement components together. This makes its dynamics more interesting than a flat plate, where the bending vibration is decoupled from the two in-plane components. The natural frequencies of a finite shell with and without smeared stiffeners will be compared. Periodic structure theory will be applied to compare the wave propagation in the plain cylindrical shell, the shell with smeared stiffener properties, and the shell with discrete stiffeners. Approaches to calculate the natural frequencies of the shell with discrete stiffeners, and to investigate the effect of some randomisation of stiffener spacing, will also be discussed.

MODELLING APPROACHES

The equations of motion for a thin cylindrical shell including the option of smeared ring stiffeners will be presented. These can then be used to calculate the natural frequencies of a cylinder of finite length, or to calculate wavenumbers for vibration propagation in an infinite periodic cylinder made up of uniform-length units of shell with or without discrete ring stiffeners at their ends.

Equations of motion

Figure 1 shows a thin cylindrical shell of radius R , thickness h and length L . Also shown is the coordinate system x (longitudinal), y (tangential) and z (radial) centred on an element of the shell surface which is at angular position θ .

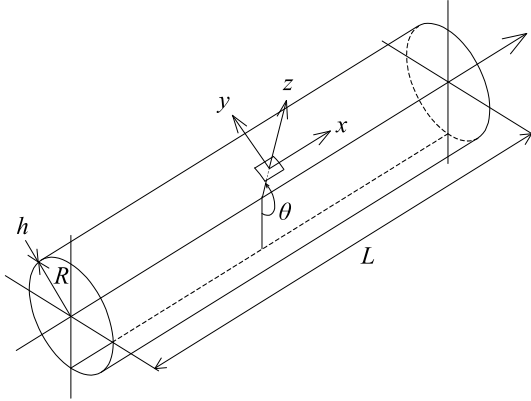


Figure 1. A thin cylindrical shell of radius R and thickness h showing the local coordinate system x , y and z used.

A cylindrical shell with ring stiffeners will be considered here. Leissa (1993b) gives results for a number of orthotropic shell formulations. When these are applied to shells with discrete stiffeners, the stiffener properties are effectively smeared over the whole shell. If the approach of Mikulas and McElman quoted in Leissa (1993b) is simplified to consider only ring stiffeners and ignore longitudinal stringers, and inertia terms and general distributed forces are also added in, the following three equations of motion for equilibrium along each coordinate result:

$$R^2 u_{xx} + (1-\nu)u_{\theta\theta}/2 - \rho(1-\nu^2)R^2 \ddot{u}/E + (1+\nu)Rv_{x\theta}/2 - \nu R w_x + (1-\nu^2)R^2 q_1/Eh = 0 \quad (1)$$

$$(1+\nu)Ru_{x\theta}/2 + (1-\nu)R^2 v_{xx}/2 + [1 + A(1-\nu^2)/ah]v_{\theta\theta} - \rho(1-\nu^2)R^2 \ddot{v}/E + [1 + A(1-\nu^2)/ah]w_{\theta} - \bar{z}A(1-\nu^2)w_{\theta\theta\theta}/ahR + (1-\nu^2)R^2 q_2/Eh = 0 \quad (2)$$

$$\nu Ru_x + [1 + A(1-\nu^2)/ah]v_{\theta} - \bar{z}A(1-\nu^2)v_{\theta\theta\theta}/ahR + [1 + A(1-\nu^2)/ah]w - 2\bar{z}A(1-\nu^2)w_{\theta\theta}/ahR + h^2 R^2 w_{xxx}/12 + [h^2/6 + J(1-\nu)/2ah]w_{xx\theta\theta} + [h^2/12R^2 + (I_{xx} + \bar{z}^2 A)(1-\nu^2)/ahR^2]w_{\theta\theta\theta\theta} + \rho(1-\nu^2)R^2 \ddot{w}/E - (1-\nu^2)R^2 q_3/Eh = 0 \quad (3)$$

where u , v and w are the displacements and q_1 , q_2 and q_3 are the external forces per unit area in the x , y and z directions respectively. These forces are set to zero to calculate natural frequencies, or free waves in the shell. They can be set to Dirac delta functions to represent point forces in the middle of the shell, but this will not be used in the following analyses. The shell and ring stiffeners are assumed to be of the same material with a Young's modulus E and Poisson's ratio ν . The ring stiffeners are placed along the cylinder with axial spacing a and the stiffener cross-section has area A , second moment of area I_{xx} , torsion constant J and its centroid is a distance of \bar{z} from the shell middle surface. The subscripts x and θ on u , v and w denote differentiation with respect to those variables, while dot denotes differentiation with respect to time.

If the stiffener properties in equations (1) to (3) are set to zero, i.e. $A = I = J = \bar{z} = 0$, then the Donnell-Mushtari equations of motion for a uniform cylindrical shell of radius R and thickness h result. In this case, ρ is the density of the shell material. When the stiffeners are included, ρ is M/h where M is the average smeared out mass per unit area of the stiffened shell, i.e. incorporating the mass of the stiffeners. If the stiffener's cross-sectional dimensions are small compared to the radius R , then the effective density is given by

$$\rho = (1 + A/ah)\rho_{material} \quad (4)$$

It can be seen from equation (1) that the only effect on the axial equilibrium equation of adding ring stiffeners is this added mass.

Other thin-shell theories such as those of Flügge include more terms than in equations (1) to (3) to better model the bending effects in shells with higher thickness-to-radius ratios. Nevertheless, these simple Donnell-Mushtari based equations still illustrate a high degree of coupling between the three displacements u , v and w .

To solve for the natural modes of a shell of finite length L , with shear-diaphragm boundary conditions (analogous to "simple support" in flat plates) at both ends, the following modal solutions

$$\begin{aligned} u &= A \cos \lambda x \cos n \theta e^{i\omega t} \\ v &= B \sin \lambda x \sin n \theta e^{i\omega t} \\ w &= C \sin \lambda x \cos n \theta e^{i\omega t} \end{aligned} \quad (5)$$

are substituted into the equations of motion, where $\lambda = m\pi/L$ with m the number of half wavelengths along the cylinder's length and n is the number of wavelengths developed around the circumference of the cylinder in the mode shape. Here ω is the natural frequency to be solved for. To solve for free waves in the shell, solutions of the form

$$\begin{aligned} u &= A e^{i\lambda x} \cos n \theta e^{i\omega t} \\ v &= B e^{i\lambda x} \sin n \theta e^{i\omega t} \\ w &= C e^{i\lambda x} \cos n \theta e^{i\omega t} \end{aligned} \quad (6)$$

are substituted, where each displacement function is described in the axial direction by a wavenumber λ which is to be solved for a given circumferential mode number n and angular frequency ω .

Substitution of solutions (5) or (6) into the equations of motion (1), (2) and (3) results in a matrix equation of the form

$$\begin{bmatrix} b_{11} & b_{12} & b_{13} \\ b_{21} & b_{22} & b_{23} \\ b_{31} & b_{32} & b_{33} \end{bmatrix} \begin{Bmatrix} A \\ B \\ C \end{Bmatrix} = \begin{Bmatrix} 0 \\ 0 \\ 0 \end{Bmatrix} \quad (7)$$

where

$$\begin{aligned} b_{11} &= \mp R^2 \lambda^2 - (1-\nu)n^2/2 + \Omega^2 \\ b_{12} &= R(1+\nu)n\lambda/2 \\ b_{13} &= R\nu\lambda \\ b_{21} &= \pm R(1+\nu)n\lambda/2 \\ b_{22} &= \mp R^2 (1-\nu)\lambda^2/2 - (1+s_A)n^2 + \Omega^2 \\ b_{23} &= -(1+s_A)n - s_z n^3 \end{aligned} \quad (8)$$

$$\begin{aligned}
 b_{31} &= \mp R \nu \lambda \\
 b_{32} &= (1 + s_A)n + s_Z n^3 \\
 b_{33} &= kR^4 \lambda^4 \pm 2kR^2(1 + s_J)n^2 \lambda^2 + k(1 + s_I)n^4 \\
 &\quad + 2s_Z n^2 + (1 + s_A) - \Omega^2
 \end{aligned} \tag{8}$$

The upper sign in equations (8) is for the natural frequency equation and the lower sign is for the free wave equation, arising from the use of trigonometric functions of λx in equation (5) versus exponentials in equation (6). The parameter k is defined as $k \equiv h^2/12R^2$ and the non-dimensional frequency squared $\Omega^2 \equiv \rho(1 - \nu^2)R^2 \omega^2/E$ is the squared ratio of the frequency to the shell ring frequency. The ring frequency is that of the “breathing” mode of the whole shell, where the wavelength of longitudinal waves is equal to the shell circumference. The shell stiffener section parameters are defined as

$$\begin{aligned}
 s_A &\equiv A(1 - \nu^2)/ah \\
 s_Z &\equiv \bar{z}A(1 - \nu^2)/Rah \\
 s_J &\equiv 3J(1 - \nu)/ah^3 \\
 s_I &\equiv 12(I_{xx} + \bar{z}^2 A)(1 - \nu^3)/ah^3
 \end{aligned} \tag{9}$$

and are all zero for a plain shell with no stiffeners smeared into it.

Calculation of natural frequencies

The natural frequencies can be determined from equation (7) based on the solutions given by equation (5). Equation (7) has a non-trivial solution when the determinant of the matrix is zero. The determinant can be expanded out explicitly in terms of the coefficients b_{ij} to give a cubic polynomial in Ω^2 . This can then be solved numerically to give three values of Ω^2 for each m, n pair. The natural frequencies are derived from the positive square roots of these values. This is the method described in Leissa (1993b) and demonstrated in Forrest (2005).

An alternative method based on eigenvalues will be used in this paper. Inspection of the coefficients (8) shows that Ω^2 appears only in the diagonal terms b_{11}, b_{22} and b_{33} . Multiplying the first two rows of (7) by -1 results in all diagonals of the matrix containing a $-\Omega^2$ term. Thus Ω^2 represents the eigenvalues of the matrix formed from the b_{ij} omitting the Ω^2 from the diagonals and with the first and second rows having their signs reversed. The eigenproblem can then be solved numerically for each m, n to give the squared natural frequencies Ω^2 as eigenvalues and the modeshapes $\{A B C\}^T$ as the eigenvectors.

Since eigenvectors are arbitrarily scaled, the ratios A/C and B/C can be considered to determine the relative amounts of motion in each direction for the mode. For example, if A/C is large and B/C is small, then the mode is predominantly axial. If both ratios are less than unity, then the mode is predominantly radial, and so on.

Calculation of free wavenumbers

Solving equation (7) for the wavenumber λ based on the solutions (6) is a different proposition. λ appears raised to various powers in several of the coefficients (8), so eigenanalysis is not applicable this time and the determinant of the matrix in (7) must be expanded out explicitly. This gives a

quartic polynomial in λ^2 which can be solved numerically to eventually give eight values of λ at a specific frequency ω and circumferential mode number n .

For each of these wavenumbers, the ratios A/C and B/C can be calculated from any two rows of the matrix in (7), since its determinant is zero when that λ value is substituted. One solution is

$$\begin{aligned}
 A_{sn}/C_{sn} &\equiv \varphi_{sn} = (-b_{13}b_{22} + b_{12}b_{23})/(b_{11}b_{22} - b_{12}b_{21}) \\
 B_{sn}/C_{sn} &\equiv \psi_{sn} = (b_{13}b_{21} - b_{11}b_{23})/(b_{11}b_{22} - b_{12}b_{21})
 \end{aligned} \tag{10}$$

where the subscript s refers to the particular wavenumber (1 to 8). Thus the coefficients A and B in solutions (6) can be written in terms of C . The total displacements at a given n can then be written as

$$\begin{aligned}
 u &= \sum_{s=1}^8 \varphi_{sn} C_{sn} e^{\lambda_{sn} x} \cos n\theta e^{i\omega t} \\
 v &= \sum_{s=1}^8 \psi_{sn} C_{sn} e^{\lambda_{sn} x} \sin n\theta e^{i\omega t} \\
 w &= \sum_{s=1}^8 C_{sn} e^{\lambda_{sn} x} \cos n\theta e^{i\omega t}
 \end{aligned} \tag{11}$$

that is, a sum of the contributions of terms due to the eight roots for λ . Each root has its negative counterpart, so the two represent a pair of waves, one travelling in the positive x -direction, the other in the negative x -direction. If solving directly for a uniform semi-infinite cylinder extending in the positive x -direction, only four of the roots for λ would thus be included in the sums (11). If there were some damping included in the model, this would mean in practice that the four roots with negative real parts would be used, so that the waves they represent decay with increasing x .

Forces acting on a periodic unit

Consider constructing an infinite cylinder from a periodic repetition of a cylinder unit of length a . To join these units together requires knowledge of the forces acting on the ends of each unit. These generalised end forces are shown in Figure 2 with the sign conventions that will be used here.

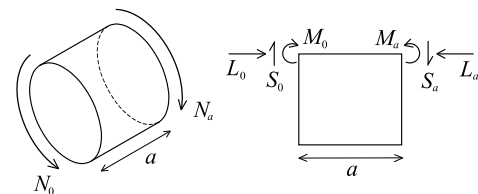


Figure 2. The forces and moments per unit length acting on the ends of one cylindrical periodic unit, isometric and side views. The forces act around the whole circumference but are only shown at the top of the right-hand figure for clarity.

Expressions for the end forces are given by Mead and Bardell (1987). These allow for stiffeners of arbitrary open, not necessarily symmetric, cross-section. If we assume a stiffener of rectangular section of width b and depth d , which is a symmetric and relatively slender section, the Wagner torsion-bending constant Γ can be taken as zero, as can the product moment of area I_{xz} . Thus the end force expressions can be simplified to the following formulae.

$$\begin{aligned}
RM_{0,a} = & \frac{Eh^3R}{12(1-\nu^2)} \left\{ w_{xx} + \frac{\nu}{R^2}(w_{\theta\theta} - v_\theta) \right\} \Big|_0^a \\
& + \frac{1}{2} \left[-\frac{EI_{zz}}{R} \left(w_x - \frac{u_{\theta\theta}}{R} \right) - \frac{EAb}{2R} (w + v_\theta) + \frac{GJ}{R} \left(w_{x\theta\theta} - \frac{u_{\theta\theta}}{R} \right) \right. \\
& \left. - R\rho \left(I_{xx} \ddot{w}_x + I_{zz} \ddot{w}_x - \frac{Ad}{2} \ddot{u} + \frac{Ab}{2} \ddot{w} \right) \right]
\end{aligned} \quad (12)$$

$$\begin{aligned}
RS_{0,a} = & -\frac{Eh^3R}{12(1-\nu^2)} \left\{ w_{xxx} + \frac{(2-\nu)}{R^2} (w_{x\theta\theta} - v_{x\theta}) \right\} \Big|_0^a \\
& + \frac{1}{2} \left[\frac{EA}{R} \left(w + v_\theta + \frac{b}{2} w_x + \frac{d}{2R} v_\theta - \frac{d}{2R} w_{\theta\theta} - \frac{b}{2R} u_{\theta\theta} \right) \right. \\
& \left. + \frac{EI_{xx}}{R^3} (w_{\theta\theta\theta} - v_{\theta\theta}) - \frac{EAd}{2R^2} (w_{\theta\theta} + v_{\theta\theta}) \right. \\
& \left. - R\rho \left(\frac{I_{xx}}{R^2} \ddot{w}_{\theta\theta} - \frac{I_{xx}}{R^2} \ddot{v}_\theta - \frac{Ad}{2R} \ddot{v}_\theta \right) + R\rho A \left(\ddot{w} + \frac{b}{2} \ddot{w}_x \right) \right]
\end{aligned} \quad (13)$$

$$\begin{aligned}
RN_{0,a} = & \frac{EhR}{2(1-\nu^2)} \left\{ (1-\nu) \left(v_x + \frac{u_\theta}{R} \right) - 4k(1-\nu)(w_{x\theta} - v_x) \right\} \Big|_0^a \\
& + \frac{1}{2} \left[-\frac{EA}{R} \left(v_{\theta\theta} + w_\theta + \frac{d}{2R} w_\theta + \frac{b}{2} w_{x\theta} + \frac{d}{R} v_{\theta\theta} \right. \right. \\
& \left. \left. - \frac{d}{2R} w_{\theta\theta\theta} - \frac{b}{2R} v_{\theta\theta} \right) + \frac{EI_{xx}}{R^3} (w_{\theta\theta\theta} - v_{\theta\theta}) \right. \\
& \left. + R\rho \left(A\ddot{u} + \frac{Ad}{R} \ddot{v} - \frac{Ad}{2R} \ddot{w}_\theta - \frac{Ab}{2R} \ddot{u}_\theta + \frac{I_{xx}}{R^2} \ddot{v} - \frac{I_{xx}}{R^2} \ddot{w}_\theta \right) \right]
\end{aligned} \quad (14)$$

$$\begin{aligned}
RL_{0,a} = & \frac{EhR}{(1-\nu^2)} \left\{ u_x + \frac{\nu}{R} (w + v_\theta) \right\} \Big|_0^a + \frac{1}{2} \left[\frac{EI_{zz}}{R} \left(\frac{u_{\theta\theta\theta}}{R^2} - \frac{w_{x\theta\theta}}{R} \right) \right. \\
& \left. - \frac{EAb}{2R^2} (w_{\theta\theta} + v_{\theta\theta}) - \frac{GJ}{R} \left(\frac{u_{\theta\theta}}{R^2} - \frac{w_{x\theta\theta}}{R} \right) \right. \\
& \left. + R\rho A \left(\ddot{u} - \frac{d}{2} \ddot{w}_x \right) - R\rho \left(\frac{I_{zz}}{R^2} \ddot{u}_{\theta\theta} - \frac{Ab}{2R} \ddot{v}_\theta \right) \right]
\end{aligned} \quad (15)$$

These are based on Love-Timoshenko shell theory, but this differs little from the Donnell-Mushtari formulation used earlier. The first term in each expression, grouped with curly brackets, represents the contribution of shell deformation to the forces. Note that it has a different sign depending on which end it is calculated for. The remaining terms represent the contribution of beam stiffener deformation to the forces. The factor of one-half outside this second group of terms in each force expression is because only half a stiffener is considered at each end of the cylinder unit.

Periodic structure calculation

The approach to the analysis of an infinitely long periodic cylinder used by Mead and Bardell (1987) and adopted here is based on the propagation of states of force and displacement along the structure. The states \mathbf{F}_0 at $x=0$ and \mathbf{F}_a at $x=a$ of a single periodic unit are defined as

$$\begin{aligned}
\mathbf{F}_0 = & \{-L_0 \quad -N_0 \quad -S_0 \quad -M_0 \quad u_0 \quad v_0 \quad w_0 \quad w_0'\}^T \\
\mathbf{F}_a = & \{L_a \quad N_a \quad S_a \quad M_a \quad u_a \quad v_a \quad w_a \quad w_a'\}^T
\end{aligned} \quad (16)$$

where the elements of these vectors are the forces and displacements as developed earlier, calculated at the ends, and dash indicates derivative with respect to x in this case (so the last element is a rotation). It is assumed that the propagation of a state from one end of a unit to the other is governed by

$$\mathbf{F}_a = e^\mu \mathbf{F}_0 \quad (17)$$

that is, the state is only changed in amplitude and phase by the complex factor e^μ as it moves down the structure. This is a statement of Floquet's theorem. The real part of the propagation constant μ thus represents the attenuation of the state along the structure.

Substituting the displacements defined in (11) into the force expressions (12) to (15) and differentiating w to get the rotation required, the end states of the cylinder unit can be written as

$$\mathbf{F}_0 = [\mathbf{K}_0] \mathbf{C}_{sn} \frac{\sin}{\cos}(n\theta) e^{i\alpha x}, \quad \mathbf{F}_a = [\mathbf{K}_a] \mathbf{C}_{sn} \frac{\sin}{\cos}(n\theta) e^{i\alpha x} \quad (18)$$

where "sin" is used for the tangential displacement $v_{0,a}$ and tangential force $N_{0,a}$ and "cos" is used for all other forces and displacements. Matrices $[\mathbf{K}_0]$ and $[\mathbf{K}_a]$ are functions of ω , n and the wavenumbers λ_{sn} . Substitution of these expressions (18) into the propagation equation (16) and some manipulation yields

$$([\mathbf{K}_0]^{-1} [\mathbf{K}_a] - e^\mu [\mathbf{I}]) \mathbf{C}_{sn} = 0 \quad (19)$$

so that the propagation constants μ can be obtained from the values of e^μ found as eigenvalues of the 8×8 matrix product $[\mathbf{K}_0]^{-1} [\mathbf{K}_a]$, a straightforward numerical operation. There are eight values of μ that come in pairs that are the negative of each other, since all eight roots λ have been considered in the underlying displacement sums (11). The members of each of these pairs represent the same manner of propagation of the state, but in opposite directions along the cylinder. Therefore, in comparing the computed attenuation factors, only four distinct values of μ need to be considered.

RESULTS

The cylindrical shell considered here is based on the plain (unstiffened) steel shell for which experimentally determined modes and natural frequencies are compared to theoretical ones in Forrest (2005), and sound radiation and active control are analysed in Forrest (2007). The shell properties and hypothetical ring stiffener properties are given in Table 1.

Table 1. Properties of the cylindrical shell and ring stiffeners

Quantity	Symbol	Value
Shell radius	R	200 mm
Shell thickness	h	2 mm
Shell length	L	1.5 m
Stiffener spacing	a	100 mm
Stiffener width	b	4 mm
Stiffener depth	d	30 mm
Young's modulus	E	210 GPa
Poisson's ratio	ν	0.3
Density	ρ	7800 kg/m ³

Other parameter values are derived from these, such as $G = E/2(1 + \nu)$, $I_{xx} = bd^3/12$ and $I_{zz} = b^3d/12$. Young and Budynas (2002) give formulae for the torsion constant J , which they denote K , for various cross-sections. For a rectangular cross-section, the torsion constant is given within 4% accuracy by

$$J = b^3d \left[\frac{1}{3} - 0.21 \frac{b}{d} \left(1 - \frac{b^4}{12d^4} \right) \right] \quad (20)$$

for the notation used here, with $d > b$.

The numerical results presented below were calculated using the Matlab software package.

Natural frequencies for plain and smeared shells

The eigenvalue method described in the previous section was used to calculate the natural frequencies of the finite cylindrical shell of length 1.5 m, for various combinations of the modal parameters m and n . The results for the plain shell without any stiffeners are given in Table 2. The results for the shell with stiffeners, calculated using the smeared shell approximation, are given in Table 3.

The natural frequencies in both tables are categorised according to their predominant nature. Nevertheless, there is always some motion in the other two directions. In a few cases, the modes have equal radial and tangential motion (A/C small and $B/C \approx 1$ within 10%) or equal axial and tangential motion ($A/C \approx B/C$ within 10% and greater than unity), and these are marked accordingly. An interesting feature of cylindrical shells that can be seen in both sets of results is that the natural frequency does not necessarily increase with modal order.

Table 2. Natural frequencies for the plain shell, * radial-tangential mode, † axial-tangential mode.

Mode shape		Natural frequency (Hz)		
m	n	radial	axial	tangential
1	1	422*	3044	6247*
	2	161	5307	9806
	3	132	7784	13792
	4	201	10311	17931
2	1	1214*	3962	6679
	2	547	5785	10193
	3	305	8072	14103
	4	263	10512	18184
3	1	1988	4830	7529†
	2	1040	6418	10844
	3	595	8507	14616
	4	417	10829	18600

Some of the higher natural frequencies given are going to be unrealistic. Even though the wavelengths, as indicated by the modal parameters m and n , are still large relative to the shell thickness, the effects of shear and rotary inertia are going to become significant at these higher rates of oscillation. These effects are ignored by all thin shell theories.

Using the cylinder parameters of Table 1 and equation (4), the smeared shell's effective density is 1.6 times the basic material density, which is the plain shell's density. If just this mass effect was added, natural frequencies would be expected to drop by a factor of the square root of 1.6, or about 20%. This is seen in some of the lower-order axial modes, where axial motion is not affected by the ring stiff-

ness as discussed earlier with respect to equation (1). As the axial mode orders become more complicated (and involve greater amounts of motion in the other coordinate directions), this reduction is less than 20%.

Table 3. Natural frequencies for the smeared shell, * radial-tangential mode.

Mode shape		Natural frequency (Hz)		
m	n	radial	axial	tangential
1	1	343*	2459	6093*
	2	418	4248	9615
	3	967	6197	13571
	4	1759	8187	17678
2	1	963*	3338	6288*
	2	584	4769	9793
	3	984	6546	13712
	4	1758	8447	17791
3	1	1590*	4280	6681
	2	916	5477	10101
	3	1061	7072	13949
	4	1771	8855	17980

For the radial modes at $n = 1$, the smeared shell has lower frequencies. This is because $n = 1$ corresponds to pure translation of the cylinder cross-section (i.e. a beam bending mode of the cylinder), so that the ring stiffeners also do not deform and just add mass. For higher values of n , the stiffening effect of the rings comes into play, and the smeared shell's natural frequencies are higher than those for the plain shell.

Propagation constants

By way of example, the propagation constants μ for infinitely long cylinders using the properties of Table 1 were calculated for $n = 4$ using equation (19). Attempts to generate the quartic polynomial in λ^2 from the matrix in equation (7) by means of calculating the determinant of a matrix of numerical polynomials in λ with the Matlab or Scilab software packages failed to give correct roots for λ . This was because the spread of numerical values of the polynomial coefficients was too great, leading to significant round-off error. Depending on the method, this sometimes resulted in only a cubic in λ^2 being generated for the characteristic determinant. Thus the determinant was expanded in full symbolically using the Maxima computer algebra system, and the resulting expressions used to set up the characteristic polynomial for numerical solution of the roots in Matlab.

Three different cases were considered: a plain shell, a smeared shell, and a shell with discrete stiffeners. These were generated using different combinations of the shell and force equations to give a specific version of (19). For the plain shell, the stiffener properties are zero for calculation of the wavenumbers λ_{sn} and only the shell terms are considered in the force expressions (12) to (15). For the smeared shell, the stiffener properties are included in the calculation of the λ_{sn} , but only the shell terms are included in the forces. For the shell with discrete stiffeners, wavenumbers are the same as for the plain shell, but the full force expressions including shell and stiffener contributions are used. No damping has been included in the modelling for these free-wave propagation results. The attenuation factors for the three cases are plotted in Figures 3, 4 and 5. The non-dimensional frequency Ω is used for the independent axis, calculated with the basic material density for all cases. For the cylinder parameters used here, the ring frequency (i.e. when $\Omega = 1$) is 4328 Hz. Thus the upper frequency limit of the plots is greater than

8 kHz, which may be beyond the range of validity of the thin-shell theory used to model the cylinders.

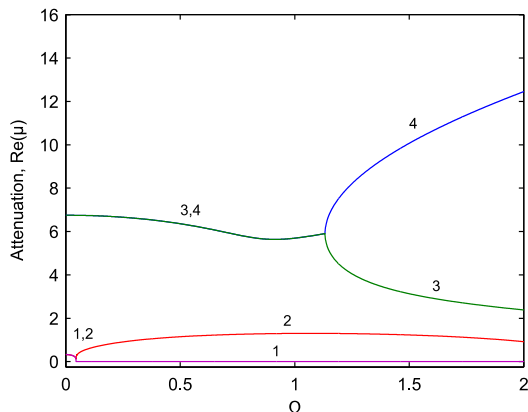


Figure 3. Attenuation factors (real part of the propagation constants) for the plain shell.

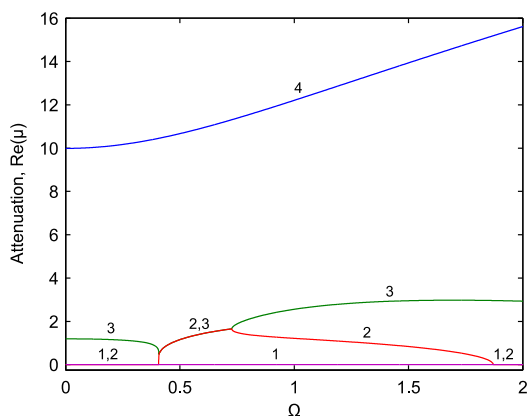


Figure 4. Attenuation factors (real part of the propagation constants) for the shell with smeared stiffener properties.

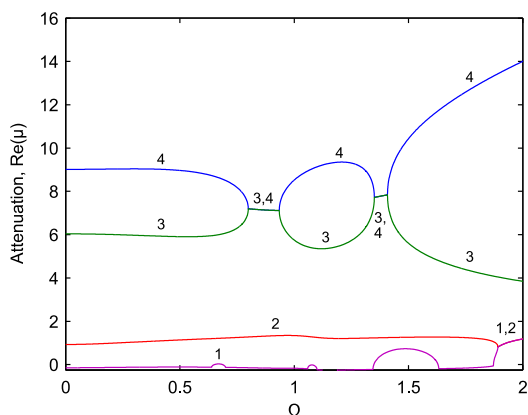


Figure 5. Attenuation factors (real part of the propagation constants) for the shell with evenly spaced discrete stiffeners.

As mentioned previously, only four of the eight propagation constants need be considered, one from each positive/negative pairing. These are marked by numbers 1 to 4 in the plots. For some frequency ranges, propagation constants are complex conjugates of one another, so overlap in the figures, since they are plots of real part only. When the attenuation is non-zero, the corresponding wave types do not

propagate indefinitely, but decay. When at least one attenuation factor is zero, propagating waves result. The frequency ranges where the latter occurs are known as pass bands, while ranges outside this are known as stop bands.

It can be seen that the three figures are different, although Figure 3 for the plain shell and Figure 5 for the shell with discrete stiffeners have some broad similarity in the upper half of the frequency range shown. In particular, the two methods for treating stiffeners (smeared or discrete) give very different results as evident in comparing Figures 4 and 5.

In Figure 3, there is a short stop band from zero to about $\Omega = 0.045$ where no waves propagate down the cylinder, because both attenuation factors 1 and 2 are non-zero. This corresponds to a frequency of 195 Hz. This represents the cut-on of the propagation of the $n = 4$ circumferential flexural ring mode down the cylinder. These cut-on frequencies for successive flexural ring modes are discussed by Forrest (2006) in the context of an infinitely long cylindrical shell representing a railway tunnel. Otherwise, attenuation factor 1 is always zero, so there is always propagation for frequencies above 195 Hz for $n = 4$ in the plain shell.

In Figure 4, attenuation factor 1 is always zero, while attenuation factor 2 is also zero for $\Omega < 0.407$ and $\Omega > 1.871$ (frequencies of 1761 Hz and 8098 Hz). Thus there is always at least one, and sometimes two, wave types propagating along the smeared shell for the frequency range shown. It is interesting that there is no low-frequency non-propagation stop band as there is for the plain shell.

The attenuation factors for the shell with discrete stiffeners shown in Figure 5 display different behaviour again. The general layout is similar to the plot given by Mead and Bardell (1987) for a small cylinder of similar configuration but different dimensions at $n = 4$. This time only attenuation factor 1 is sometimes zero, with a number of non-zero stop bands appearing. While again there is no low-frequency stop band corresponding to that in the plain shell, there are stop bands at $0.639 < \Omega < 0.700$ (2766 Hz to 3030 Hz frequency), $1.058 < \Omega < 1.100$ (4579 Hz to 4761 Hz), $1.344 < \Omega < 1.633$ (5817 Hz to 7068 Hz) and $\Omega > 1.871$ (8098 Hz). The pass band parts of factor 1 are not exactly zero, which suggests some numerical issue or a mismatch due to the different shell theories used to calculate the free wavenumbers on the one hand and the end forces and moments on the other. However, the overall picture is clear. In contrast to the smeared shell results, consideration of discrete stiffeners shows that there are stop bands where no propagation occurs, and that when there are pass bands, only one wave type, never two, propagates along the cylinder.

DISCUSSION

Consideration of the propagation constants and the attenuation factors that are their real parts illustrate some of the differences in the two approaches to including stiffeners in a cylindrical shell. However, they do not alone make it clear as to when the simpler smeared shell approach is appropriate for practical modelling of a cylinder. While the non-zero attenuation factors in Figures 3 to 5 differ a lot, their corresponding waves may not have much influence on a total displacement field in a cylinder under forced vibration simply because these waves will not be propagating. Another way of looking at this is that any given arbitrary state can be written as a unique linear combination of the eigenstates C_{sn} from equation (19), each governed by its own μ value. The two different models will have different sets of eigenstates but there-

fore also different linear combinations to represent the same arbitrary state, so that the propagation of the overall total state may be much the same in both. Additionally, the stop bands that appear when discrete stiffeners are considered only occur at relatively high frequencies. The effects on natural frequencies are also not immediately obvious.

Natural frequencies for a discretely stiffened shell

Mead and Bardell (1987) describe a method to estimate the natural frequencies for a finite-length stiffened shell based on the phase of the propagation constants μ . This method is taken to be valid for cylinders with simply supported (shear diaphragm) or clamped ends. The method is based on the idea that a wave impinging on one of these boundary types will suffer a phase change of $\pm\pi$ on reflection. Say the finite cylinder comprises N cylindrical units as defined previously. The phase axis is conceptually divided into N equal intervals between 0 and $\pm\pi$ and horizontal lines of constant phase are drawn at these divisions. The natural frequencies are estimated as the intersections of these horizontal lines with the curves of the phase of the propagation constants μ .

In practice, these intersections on the phase curve would be solved numerically, and would have to be done for the phase curves calculated over a range of n values. The natural frequencies could then be compared to those in Tables 2 and 3. However, the issues described for the results of Figure 5 for the current shell with discrete stiffeners would need to be resolved to ensure reasonable accuracy of estimated frequencies.

Finite shell with discrete stiffeners

The expressions given in equation (18) for the states of force and displacement at the ends of a unit of cylinder can be used in a slightly different way. Instead of writing the equations in terms of the end states \mathbf{F}_0 and \mathbf{F}_a , one matrix equation can be written for all the end displacements and one for all the end forces in terms of the constants \mathbf{C}_{sn} . This allows the elimination of those constants to generate a dynamic-stiffness matrix instead of the propagation matrix product $[\mathbf{K}_0]^{-1}[\mathbf{K}_a]$.

The dynamic-stiffness matrix relates the forces (at both ends) to the displacements (at both ends). As such, it can be assembled with the dynamic-stiffness matrices of other structural elements in the same way as stiffness matrices are assembled in the finite-element method. However, such dynamic-stiffness matrices describe much larger parts of a structure than a finite element does, so the order of the matrix representation of the structural dynamics is still relatively small.

This approach could be used to link a number of cylinder units together and the forced response could be calculated. This would require the summation of contributions over a range of n values to generate a total response to a general set of forces.

Randomisation of stiffener spacing

It would be interesting to investigate the effect of stiffeners with random spacing on the wave propagation and forced response. This could be based on the uniform spacing already considered with say $\pm 20\%$ variation in the axial placement of the stiffeners, while keeping the overall length of the cylindrical shell the same.

Dynamic-stiffness matrices could be generated for a number of cylindrical units with varying lengths matching the different stiffener spacings. These could then be assembled as described in the previous section above. This could be used to calculate forced responses. Alternatively, this newly assembled dynamic-stiffness matrix could be partitioned and rearranged to go back to a propagation matrix relating end states, but now for a longer cylindrical unit with a number of randomly spaced stiffeners included. Solving for the eigenvalues of this new matrix would give the propagation constants μ for a "pseudo-random" infinitely long stiffened cylinder, where the randomness of the stiffener spacing repeats periodically. These new μ values could then be compared with those calculated for a cylinder with uniformly spaced discrete stiffeners as presented in this paper.

CONCLUSIONS

The dynamics of a plain cylindrical shell and a cylindrical shell with ring stiffeners have been considered. The stiffened shell has been treated via two approaches: the smearing of the mass and stiffness of the ring stiffeners into the continuous shell, and the consideration of discrete stiffeners using periodic structure theory.

Comparison of the natural frequencies calculated for a finite plain shell and a finite shell with smeared stiffeners shows expected effects of the ring stiffeners. Modes that are predominantly axial in nature are reduced in natural frequency in proportion with the mass added by the stiffeners, especially at lower circumferential orders, as the stiffeners are not being deformed much so only their mass counts. Modes that have significant radial motion are raised in frequency because the stiffness of the rings is the significant factor this time, and this is a bigger effect than the added mass for the parameter values chosen for this paper.

Propagation constants calculated from periodic structure theory show some distinct differences between the plain shell, smeared shell and shell with discrete stiffeners. The curves of the non-zero attenuation factors corresponding to non-propagating waves vary quite a lot between the three cases. Propagation behaviour is also different. The plain shell exhibits a small stop band from zero to the cut-on frequency of the flexural ring mode for the $n = 4$ case calculated. Neither of the stiffened shell models exhibit this. The smeared shell always has at least one wave type propagating over the frequency range calculated, and sometimes has two. The shell with discrete stiffeners shows four stop bands, but at higher frequency ranges. In its pass bands, it only ever has one propagating wave type.

A number of areas for future work could shed light on the importance of the differences between the smeared and discrete stiffener models. The phase of the propagation constants could be used to estimate the natural frequencies of a finite shell with discrete stiffeners, and these could be compared to the ones calculated in this paper for the smeared shell. Some of the analysis used for the periodic structure could be modified to create a dynamic-stiffness matrix of a typical cylindrical shell unit. A number of these units could then be assembled as in the finite-element method and the forced response calculated. This approach would also be amenable to modelling the effects of some randomisation of stiffener spacing.

REFERENCES

- Efimov, BM and Lazarev, LA (2009), 'Forced vibrations of plates and cylindrical shells with regular orthogonal system of stiffeners', *Journal of Sound and Vibration*, 327(1-2), 41-54.
- Forrest, JA (2005), 'Measured dynamics of a thin cylindrical shell subject to axial excitation', *Proceedings of Acoustics 2005*, 9-11 November 2005, Busselton, Western Australia, pp. 61-66.
- Forrest, JA and Hunt, HEM (2006), 'A three-dimensional tunnel model for calculation of train-induced ground vibration', *Journal of Sound and Vibration*, 294(4), 678-705.
- Forrest, JA (2007), 'Moment control of the sound radiated from an axially excited cylindrical shell', *Proceedings of 14th International Congress on Sound and Vibration (ICSV14)*, 9-12 July 2007, Cairns, Australia.
- Gan, L, Li, X and Zhang, Z (2009), 'Free vibration analysis of ring-stiffened cylindrical shells using wave propagation approach', *Journal of Sound and Vibration*, 326(3-5), 633-646.
- Hodges, CH, Power, J & Woodhouse, J (1985), 'The low frequency vibration of a ribbed cylinder, part 1: theory', *Journal of Sound and Vibration*, 101(2), 219-235.
- Junger, MC & Feit, D (1993), *Sound, Structures and Their Interaction*, 2nd ed., Acoustical Society of America, New York.
- Langley, RS (1989), 'Application of the dynamic stiffness method to the free and forced vibrations of aircraft panels', *Journal of Sound and Vibration*, 135(2), 319-331.
- Lee, J-H and Kim, J (2002), 'Sound transmission through periodically stiffened cylindrical shells', *Journal of Sound and Vibration*, 251(3), 431-456.
- Leissa, A (1993a), *Vibration of Plates*, Acoustical Society of America, New York.
- Leissa, A (1993b), *Vibration of Shells*, Acoustical Society of America, New York.
- Luan, Y, Ohrlich, M and Jacobsen, F (2011), 'Improvements of the smearing technique for cross-stiffened thin rectangular plates', *Journal of Sound and Vibration*, 330(17), 4274-4286.
- Mace, BR (1980), 'Periodically stiffened fluid-loaded plates, II: response to line and point forces', *Journal of Sound and Vibration*, 73(4), 487-504.
- Mead, DJ & Bardell, NS (1986), 'Free vibration of a thin cylindrical shell with discrete axial stiffeners', *Journal of Sound and Vibration*, 111(2), 229-250.
- Mead, DJ & Bardell, NS (1987), 'Free vibration of a thin cylindrical shell with periodic circumferential stiffeners', *Journal of Sound and Vibration*, 115(3), 499-520.
- Ruotolo, R (2002), 'Influence of some thin shell theories on the evaluation of the noise level in stiffened cylinders', *Journal of Sound and Vibration*, 255(4), 777-788.
- Solaroli, G, Gu, Z, Baz, A and Ruzzene, M (2003), 'Wave propagation in periodic stiffened shells: spectral finite element modeling and experiments', *Journal of Vibration and Control*, 9(9), 1057-1081.
- Young, WC and Budynas, RG (2002), *Roark's Formulas for Stress and Strain*, 7th edition, McGraw-Hill, New York.